Monthly Notices
of the
ROYAL ASTRONOMICAL SOCIETY

Mon. Not. R. Astron. Soc. **405,** 2639–2650 (2010) doi:10.1111/j.1365-2966.2010.16647.x

Understanding the origin of CMB constraints on dark energy

H. K. Jassal,[1⋆] J. S. Bagla[1⋆] and T. Padmanabhan[2⋆]

[1]*Harish-Chandra Research Institute, Chhatnag Road, Jhunsi, Allahabad 211019, India*
[2]*Inter University Centre for Astronomy and Astrophysics, Post Bag 4, Ganeshkhind, Pune 411007, India*

Accepted 2010 March 8. Received 2010 February 1; in original form 2009 June 4

ABSTRACT

We study the observational constraints of cosmic microwave background (CMB) temperature and polarization anisotropies on models of dark energy, with special focus on models with variation in properties of dark energy with time. We demonstrate that the key constraint from CMB observations arises from the location of acoustic peaks. An additional constraint arises from the limits on $\Omega_{\rm NR}$ from the relative amplitudes of acoustic peaks. Further, we show that the distance to the last scattering surface is not how the CMB observations constrain the combination of parameters for models of dark energy. We also use constraints from supernova observations and show that unlike the gold and silver samples, the Supernova Legacy Survey (SNLS) sample prefers a region of parameter space that has a significant overlap with the region preferred by the CMB observations. This is a verification of a conjecture made by us in an earlier work. We discuss combined constraints from *Wilkinson Microwave Anisotropy Probe* 5-yr and SNLS observations. We find that models with $w \simeq -1$ are preferred for models with a constant equation-of-state parameters. In case of models with a time-varying dark energy, we show that constraints on evolution of dark energy density are almost independent of the type of variation assumed for the equation-of-state parameter. This makes it easy to get approximate constraints from CMB observations on arbitrary models of dark energy. Constraints on models with a time-varying dark energy are predominantly due to CMB observations, with supernova constraints playing only a marginal role.

Key words: cosmic background radiation – cosmological parameters.

1 INTRODUCTION

Observational evidence for accelerated expansion in the Universe has been growing in the last two decades (Efstathiou, Sutherland & Maddox 1990; Ostriker & Steinhardt 1995; Bagla, Padmanabhan & Narlikar 1996). Independent confirmation using observations of high-redshift supernovae (SNe) (Garnavich et al. 1998; Perlmutter et al. 1999; Tonry et al. 2003; Barris et al. 2004; Riess et al. 2004; Astier et al. 2005) has made this result more acceptable to the community. Using these observations along with observations of cosmic microwave background (CMB) radiation (Melchiorri et al. 2000; Spergel et al. 2003; Komatsu et al. 2009) and large-scale structure (Percival et al. 2007), we can construct a 'concordance' model for cosmology and study variations around it (e.g. see Bridle et al. 2003; Tegmark et al. 2004; Dunkley et al. 2008; Komatsu et al. 2009; for an overview of our current understanding, see Padmanabhan 2005b,d,e).

Observations indicate that the dominant component of energy density – called dark energy – should have an equation-of-state parameter $w \equiv P/\rho < -1/3$ for the universe to undergo accelerated expansion. Indeed, present-day observations require $w \simeq -1$. The cosmological constant is the simplest explanation for accelerated expansion (Weinberg 1989; Carroll, Press & Turner 1992; Sahni & Starobinsky 2000; Ellis 2003; Padmanabhan 2003; Peebles & Ratra 2003; Padmanabhan 2005a; Perivolaropoulos 2006; Copeland, Sami & Tsujikawa 2006) and it is known to be consistent with observations. In order to avoid theoretical problems related to cosmological constant (Weinberg 1989; Carroll et al. 1992), many other scenarios have been investigated: these include quintessence (de la Macorra & Piccinelli 2000; Urena-Lopez & Matos 2000; de Ritis & Marino 2001; Bludman & Roos 2002; Gonzalez-Diaz 2002; Rubano & Scudellaro 2002; Sen & Seshadri 2003; Steinhardt 2003), k-essence (Armendariz-Picon, Mukhanov & Steinhardt 2001; Chiba 2002; Malquarti et al. 2003; Chimento & Feinstein 2004; Scherrer 2004), tachyon field (Choudhury et al. 2002; Frolov, Kofman & Starobinsky 2002; Gibbons 2002; Padmanabhan 2002; Shiu & Wasserman 2002; Bagla, Jassal & Padmanabhan 2003; Gibbons 2003; Kim, Kim & Kim 2003; Sen 2005; Aguirregabiria & Lazkoz 2004; Gorini et al. 2004; Jassal 2004), chaplygin gas and its generalizations (Gorini et al. 2001; Bento, Bertolami & Sen 2002; Dev, Jain & Alcaniz 2003; Sen & Scherrer 2005), phantom fields (Caldwell 2002; Onemli & Woodard

⋆E-mail: hkj@hri.res.in (HKJ); jasjeet@hri.res.in (JSB); nabhan@iucaa.ernet.in (TP)

2002; Carroll, Hoffman & Trodden 2003; Frampton 2004; Gibbons 2003; Hao & Li 2003; Nojiri & Odinstov 2003; Singh, Sami & Dadhich 2003; Gonzalez-Diaz 2003; Dabrowski, Stachowiak & Szydlowski 2003; Cline, Jeon & Moore 2004; Elizalde, Nojiri & Odintsov 2004; Nojiri, Odintsov & Tsujikawa 2005; Briscese et al. 2007; Bronnikov, Fabris & Gonçalves 2007; Bronnikov & Starobinsky 2007), branes (Uzawa & Soda 2001; Jassal 2003; Burgess 2003; Milton 2003; Gonzalez-Diaz 2000; Sahni & Shtanov 2003) and many others (Holman & Naidu 2004; Onemli & Woodard 2004; Padmanabhan 2005c, 2002; Andrianov, Cannata & Kamenshchik 2005; Lazkoz, Neseseris & Perivolaropoulos 2006; Cognola et al. 2006; Ren & Meng 2006; Polarski & Ranquet 2005; Sola & Stefancic 2006; Das, Banerjee & Dadhich 2006; Apostolopoulos & Tetradis 2006; Arianto et al. 2007; Sahni, Shafieloo & Starobinsky 2008). In these models one can have $w \neq -1$ and in general w varies with redshift. For references to papers that discuss specific models, the reader may consult one of the many reviews (Sahni & Starobinsky 2000; Padmanabhan 2003; Peebles & Ratra 2003; Ellis 2003; Padmanabhan 2005a; Alcaniz 2006). Even though these models have been proposed to overcome the fine-tuning problem for cosmological constant, most models require similar fine-tuning of parameter(s) to be consistent with observations. Nevertheless, they raise the possibility of $w(z)$ evolving with time (or it being different from -1), which can be tested by observations.

Given that w for dark energy should be smaller than $-1/3$ for the Universe to undergo accelerated expansion, the energy density of this component changes at a much slower rate than that of matter and radiation. (Indeed, $w = -1$ for cosmological constant and in this case the energy density is a constant.) Unless w is a rapidly varying function of redshift and becomes $w \sim 0$ at $z \sim 1$, the energy density of dark energy should be negligible at high redshifts ($z \gg 1$) compared to that of non-relativistic matter. If dark energy evolves in a manner such that its energy density is comparable to, or greater than the matter density in the universe at high redshifts, then the basic structure of the cosmological model needs to be modified. We do not consider such models, instead we confine our attention to constraints on dark energy in realistic models and choose observations which are sensitive to evolution of $w(z)$ at redshifts $z \leq 1$.

SN observations permit a large variation in the equation of state (Alam et al. 2004a,b). It has recently been argued that a cosmological constant with a small curvature can be interpreted as a dynamical dark energy model (Clarkson, Cortês & Bassett 2007; Virey et al. 2005). We have shown that a combination of SN observations with CMB observations and abundance of rich clusters of galaxies provides tight constraints on variation of dark energy (Jassal, Bagla & Padmanabhan 2005; Jassal, Bagla & Padmanabhan 2005a). Of these CMB data provide the most stringent bounds on the allowed variation in evolution of dark energy density. In this paper the main motivation is to study how these models fare in the light of current CMB data (Dunkley et al. 2008; Komatsu et al. 2009).

A variety of observations can be used to constrain models of dark energy, e.g. see section II B of Jassal et al. (2005a) for an overview. Observations of high-redshift SNe provided the first direct evidence for accelerated expansion of the universe (Riess et al. 1998; Perlmutter et al. 1999). This, coupled with the ease with which the high-redshift SN data can be compared with cosmological models, has made it the favourite benchmark for comparison with models of dark energy. It is often considered sufficient to compare a model with the SN data even though observers and theorists have pointed out potential problems with the data (Perlmutter & Schmidt 2003; Jain & Ralston 2006) as well as some peculiar implications of the data (Padmanabhan & Choudhury 2003; Choudhury & Padmanabhan 2005; Gupta et al. 2009). Further, it has been shown that other observations like temperature anisotropies in the CMB fix the distance to the last scattering surface and are a reliable probe of dark energy (Eisenstein & White 2004; Jassal et al. 2005). In this paper, we try to understand the origin of the constraint on models of dark energy from CMB anisotropy observations. We show that the angular scale of acoustic peaks provides the leading constraint on the combination of parameters. An additional constraint comes in through the degeneracy with $\Omega_{\rm NR}$, where a constraint on $\Omega_{\rm NR}$ from the relative heights of acoustic peaks translates into an indirect constraint on the equation-of-state parameter w.

In an earlier work, we compared the constraints on models of dark energy from SN and CMB observations and pointed out that models preferred by these observations lie in distinct parts of the parameter space and there is no overlap of regions allowed at 68 per cent confidence level (Jassal et al. 2005a). Even though different observational sets are sensitive to different combinations of cosmological parameters, we do not expect models favoured by one observation to be ruled out by another when such a divergence is not expected. This divergence may point to some shortcomings in the model, or to systematic errors in observations, or even to an incorrect choice of priors. We suggested that this may indicate unresolved systematic errors in one of the observations, with SN observations being more likely to suffer from this problem due to the heterogeneous nature of the data sets available at the time. In Supernova Legacy Survey (SNLS) (Astier et al. 2005), a concerted effort has been made to reduce systematic errors by using only high-quality observations. The systematic uncertainties are reduced by using a single instrument to observe the fields. Using a rolling search technique ensures that sources are not lost and data are of superior quality (for details see Astier et al. 2005). If our claim about gold + silver data set were to be true, SNLS data should not be at variance with the *Wilkinson Microwave Anisotropy Probe* (*WMAP*) data.[1] In this paper we study constraints on dark energy models from high-redshift SN observations from the SNLS survey and also observations of the temperature and polarization anisotropies in the CMB using the *WMAP* 5-yr (*WMAP*5) data.

This paper is a revised version of an earlier manuscript which became out of date after *WMAP*3 and then *WMAP*5 data were released. In the interim period, the issue of systematics in inhomogeneous data sets has been accepted; therefore we do not emphasize that aspect much in this version. The focus of this paper is twofold: to study constraints on dark energy models in light of the SNLS and *WMAP*5 data, and, to understand the combination of cosmological parameters that is constrained by the CMB observations.

2 DARK ENERGY

2.1 Cosmological equations

If we assume that each of the constituents of the homogeneous and isotropic universe can be considered to be an ideal fluid, and that the space is flat, the Friedman equations can be written as

$$\left(\frac{\dot{a}}{a}\right)^2 = \frac{8\pi G}{3}\rho \tag{1}$$

[1] This has been shown by several authors, including ourselves in a much earlier version of this manuscript.

and

$$\frac{\ddot{a}}{a} = -\frac{4\pi G}{3}(\rho + 3P), \tag{2}$$

where P is the pressure and $\rho = \rho_{\rm NR} + \rho_\gamma + \rho_{\rm DE}$ with the respective terms denoting energy densities for non-relativistic matter, for radiation/relativistic matter and for dark energy. Pressure is zero for the non-relativistic component, whereas radiation and relativistic matter have $P_\gamma = \rho_\gamma/3$. If the cosmological constant is the source of acceleration, then $\rho_{\rm DE} =$ constant and $P_{\rm DE} = -\rho_{\rm DE}$. Analysis of non-flat cosmologies reveals that allowed range of curvature of the universe $\Omega_{\rm K}$ is -0.012 to 0.009 at 95 per cent confidence level and a flat universe is a good fit to the current data (Xia et al. 2008).

An obvious generalization is to consider models with a constant equation-of-state parameter $w \equiv P/\rho =$ constant. One can, in fact, further generalize to models with a varying equation-of-state parameter $w(z)$. Since a function is equivalent to an infinite set of numbers (defined e.g. by a Taylor–Laurent series coefficients), it is clearly not possible to constrain the form of an arbitrary function $w(z)$ using a finite number of observations. One possible way of circumventing this issue is to parametrize the function $w(z)$ by a finite number of parameters and try to constrain these parameters with the available observational data. There have been many attempts to describe varying dark energy with different parametrizations (Wang & Tegmark 2004; Bassett et al. 2004; Jassal et al. 2005; Lee 2005; Li 2004; Hannestad & Mortsell 2004; Jassal et al. 2005a) where the functional form of $w(z)$ is fixed and the variation is described with a small number of parameters. Observational constraints depend on the specific parametrization chosen, but it should be possible to glean some parametrization independent results from the analysis.

To model varying dark energy we use two parametrizations:

$$w(z) = w_0 + w'(z=0)\frac{z}{(1+z)^p}; \quad p = 1, 2. \tag{3}$$

These are chosen so that, among other things, the high-redshift behaviour is completely different in these two parametrizations Jassal et al. (2005). If $p = 1$, the asymptotic value $w(\infty) = w_0 + w'(z=0)$ and for $p = 2$, $w(\infty) = w_0$. For both $p = 1, 2$, the present value $w(0) = w_0$. Clearly, we must have $w(z \gg 1) \leq -1/3$ for the standard cosmological models with a hot big bang to be valid. This restriction is imposed over and above the priors used in this paper.

The allowed range of parameters w_0 and $w_0' \equiv w'(z=0)$ is likely to be different for different p. However, the allowed variation at low redshifts in $\rho_{\rm DE}$ should be similar in both models as observations actually probe the variation of dark energy density.

2.2 Observational constraints

2.2.1 Supernova data

In this paper, we concentrate on SN and *WMAP* observations. SN data provide geometric constraints for dark energy evolution. These constraints are obtained by comparing the predicted luminosity distance to the SN with the observed one. The theoretical model and observations are compared for luminosity measured in magnitudes:

$$m_B(z) = \mathcal{M} + 5\log_{10}(D_{\rm L}), \tag{4}$$

where $\mathcal{M} = M - 5\log_{10}(H_0)$ and $D_{\rm L} = H_0 d_{\rm L}$, M being the absolute magnitude of the object and $d_{\rm L}$ is the luminosity distance

$$d_{\rm L} = (1+z)a(t_0)r(z); \quad r(z) = c\int \frac{{\rm d}z}{H(z)}, \tag{5}$$

where z is the redshift. This depends on evolution of dark energy through $H(z)$. For our analysis we use the SNLS data set (Astier et al. 2005) and for reference we also used the combined *gold* and *silver* SN data set in Riess et al. (2004) (see also Nesseris & Perivolaropoulos 2006). These data are a collection of SN observations from Tonry et al. (2003), Garnavich et al. (1998) and many other sources with 16 SNe discovered with *Hubble Space Telescope* (*HST*) (Riess et al. 2004). The parameter space for comparison of models with SN observations is small and we do a dense sampling of the parameter space.

2.2.2 CMB data

CMB anisotropies constrain dark energy in two ways, through the distance to the last scattering surface and through the integrated Sachs–Wolfe (ISW) effect (Peiris & Spergel 2000). Given that the physics of recombination and evolution of perturbations does not change if $w(z)$ remains within some *safe limits*, any change in the location of peaks will be due to dark energy (Eisenstein & White 2004). For models with a variable $w(z)$, the constraint is essentially on an effective value $w_{\rm eff}$ (Jassal et al. 2005a). This constraint can arise either through the angular diameter distance or the angular size of the acoustic horizon seen reflected in the scale corresponding to the acoustic peaks in the CMB angular power spectrum.

Fig. 1 shows contours of equal angular diameter distance to the last scattering surface in the $\Omega_{\rm NR}$–w plane. We assumed a fixed value of H_0 and $\Omega_{\rm B}$ for this plot. If the distance to the last scattering surface is the key constraint on models of dark energy, then the likelihood contours should run along the contours of constant distance in this plane.

We may use the angular size of the Hubble radius at the time of decoupling as an approximate proxy for the angular size of the acoustic horizon for the purpose of this discussion. The approximate angular size θ of the Hubble radius at the time of decoupling can

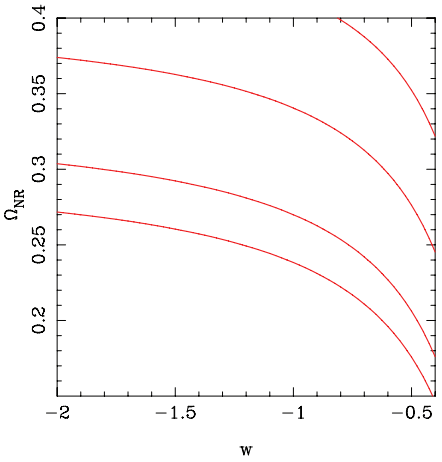

Figure 1. Contours of angular diameter distance. The range plotted is the range allowed by *WMAP*5 data. From the line on to the one at bottom the values correspond to $d_A = 12\,000,\ 13\,000,\ 14\,273,\ 20\,000$ and $20\,100$ Mpc.

be written as

$$\theta^{-1} = \frac{H_0/H(z)}{\int_0^z \mathrm{d}y/[H(y)/H_0]} \simeq \frac{\left[\Omega_{\rm NR}(1+z)^3\right]^{-1/2}}{\int_0^z \mathrm{d}y/\sqrt{\Omega_{\rm NR}(1+z)^3 + \varrho^{DE}(z)/\varrho_0^{DE}}} \equiv \frac{\left[\Omega_{\rm NR}(1+z)^3\right]^{-1/2}}{\int_0^z \mathrm{d}y/\sqrt{\Omega_{\rm NR}(1+z)^3 + \Omega_{\rm DE}(1+z)^{3(1+w_{\rm eff})}}}. \quad (6)$$

Clearly, the value of the integral will be different if we change w_0 and $w'(z=0)$, and there will also be some dependence on the parametrized form. If the location of peaks in the angular power spectrum of the CMB provide the main constraint, this can only constrain $w_{\rm eff}$ and not all of w_0, $w'(z=0)$ and p. Therefore if the present value $w_0 < w_{\rm eff}$, then it is essential that $w'(z=0) > 0$, and similarly if $w_0 > w_{\rm eff}$, then $w'(z=0) < 0$ is needed to ensure that the integrals match. Specifically, the combination of w_0, $w'(z=0)$ and p should give us $w_{\rm eff}$ within the allowed range.

Fig. 2 shows contours of constant θ in the $\Omega_{\rm NR}$–w plane. If the angular scale of acoustic peaks is the key constraint arising from CMB observations for models of dark energy, then we should see two features in the likelihood contours.

(i) Likelihood contours for models with a constant equation-of-state parameter w in the $\Omega_{\rm NR}$–w plane should run along contours of constant θ, as shown in Fig. 2.

(ii) Likelihood contours for different models of varying dark energy should coincide in the $\Omega_{\rm NR}$–$w_{\rm eff}$ plane. These should also coincide with the contours for models with a constant w in the $\Omega_{\rm NR}$–w plane.

The origin of the CMB constraints on dark energy therefore is not in the raw distance to the surface of last scattering but in the combination of parameters that determines the location of peaks in the angular power spectrum. It is important to note that the distance to the surface of last scattering is a derived quantity. The CMB observations constrain only one number, the effective equation of state. There is no ambiguity except for models with early dark energy (Linder & Robbers 2008). In these models, the growth of perturbations is slower than models in which dark energy comes into play at late times (Benabed & Bernardeau 2001; Doran & Robbers 2006).

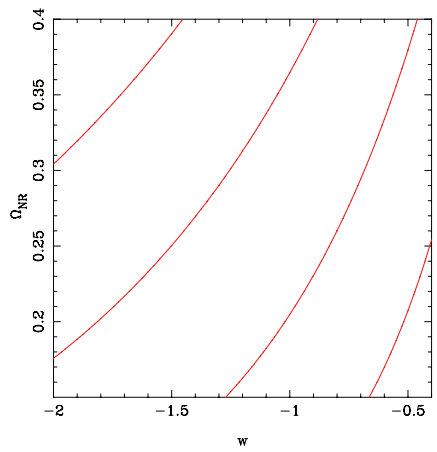

Figure 2. Contours of constant angular size of the Hubble radius. The contours from left- to right-hand side correspond to $\theta^{-1} = 0.0165$, 0.017, 0.18 and 0.020.

In our analysis, we use the angular power spectrum of the CMB temperature anisotropies (Hu & Dodelson 2002; White & Cohn 2002; Subramanian 2004) as observed by *WMAP* (Dunkley et al. 2008; Komatsu et al. 2009) and these are compared to theoretical predictions using the likelihood program provided by the *WMAP* team (Dunkley et al. 2008; Komatsu et al. 2009). We vary the amplitude of the spectrum till we get the best fit with *WMAP* observations. The CMBFAST[2] package (Seljak & Zaldarriaga 1996) is used for computing the theoretical angular power spectrum for a given set of cosmological parameters. We have combined the likelihood program with the CMBFAST code and this required a few minor changes in the CMBFAST driver routine. We also made changes in the driver program to implement Monte Carlo Markov Chain (MCMC) for sampling the parameter space. Please see (Jassal et al. 2005a) for details of the MCMC implementation.

Although we can use other observations like abundance of rich clusters, baryonic features in the power spectrum, etc. but we find that the two observations used here are sufficient for this paper (Jassal, in preparation).

3 RESULTS

In this section we will describe the results of this paper. We studied models in three classes.

(i) Models with a constant equation-of-state parameter w. We studied models with perturbations in dark energy (Bean & Doré 2004; Caldwell, Dave & Steinhardt 1998; Weller & Lewis 2003; Hannestad 2005; Fabris, Shapiro & Solà 2007; Fabris & Gonçalves 2006; Unnikrishnan, Jassal & Seshadri 2008; Jassal 2009; Bartolo et al. 2004; Mota & van de Bruck 2004; Gordon & Hu 2004; Gordon & Wands 2005; Nunes & Mota 2006; Sergijenko et al. 2008; Hu 2005; Mainini 2009, 2008) as well as without.

(ii) Models with a varying equation-of-state parameter w, with variation given by equation (3) ($p = 1$). Perturbations in dark energy were not taken into account in this case.

(iii) Models with a varying equation-of-state parameter w, with variation given by equation (3) ($p = 2$). Perturbations in dark energy were not taken into account in this case too.

We analyse the allowed range of cosmological parameters for these cosmologies and consider the probability with which the Lambda cold dark matter (ΛCDM) model is allowed within these three classes of models. In light of the significant disagreement between the allowed range of parameters from the high-redshift SN data from the gold + silver set and the CMB anisotropies from *WMAP* observations (Jassal et al. 2005a; Nesseris & Perivolaropoulos 2006), we also check the degree of overlap between the parameter space allowed by the SN and the CMB observations, respectively. The newly released 'Union' data set includes data from the SNLS, the ESSENCE Survey (Wood-Vasey et al. 2007) and the extended distant SN data set from *HST* along with the older data sets (Kowalski et al. 2008). The combined data favour variation in dark energy equation of state.

3.1 Cosmological constant

We begin with a very brief review of constraints on parameters in the case where a cosmological constant is the source of accelerating expansion of the universe. We used priors given in Table 1, except

[2] http://www.cmbfast.org

Table 1. The priors used in this paper. Apart from the range of parameters listed in the table, we assumed that the universe is flat. We assumed that the primordial power spectrum had a constant index. Further, we ignored the effect of tensor perturbations. The range of values for w_0 and $w'(z = 0)$ is as given, but with the constraint that $w(z = 1000) \leq -1/3$. Any combination of w_0 and $w'(z = 0)$ that did not satisfy this constraint was not considered. Values given in parenthesis were used for analysing constraints from high-redshift supernovae in Section 3.1.

Parameter	Lower limit	Upper limit
$\Omega_{\rm B}$	0.03	0.06
$\Omega_{\rm NR}$	0.1	0.5(0.7)
h	0.6	0.8
τ	0.0	0.4
n	0.86	1.10
w_0	$-2.0(-4.0)$	-0.4
$w'(z = 0)$	-5.0	5.0

that the equation-of-state parameter is fixed to $w = -1$. Constraints on cosmological parameters are listed in Table 2. We would like to note that our results match those obtained by other authors (Dunkley et al. 2008; Komatsu et al. 2009). Fig. 3 shows contours of likelihood for some pairs of parameters as an example. We have shown contours in the n–$\Omega_{\rm NR}h^2$, n–$\Omega_{\rm B}h^2$ and n–τ planes. There is a strong correlation between n–$\Omega_{\rm B}h^2$. These likelihood contours have also been shown as a reference for equivalent plots for models with $w \neq -1$, and help in checking the effect of the additional dark energy parameters on allowed range of other parameters.

3.2 Constant w

We first evaluate the nature of the CMB constraint on models of dark energy. Fig. 4 shows likelihood contours from *WMAP*5 observations in the $\Omega_{\rm NR}$–w plane for constant w models. We find that the orientation of these contours is roughly along contours of constant θ. To illustrate this, we have overlaid contours from Figs 1 and 2 in Fig. 4. On the other hand, there is no similarity between the likelihood and contours of distance to the last scattering surface. Thus we may conclude that the dominant constraint provided by the CMB observations arises from the location of peaks in the angular power spectrum. The reason for this is that the angular diameter distance to the last scattering surface is a derived quantity, whereas the location of peaks in the angular power spectrum of temperature anisotropies is a direct observable.

We use priors given in Table 1 for models with a constant equation-of-state parameter, with the obvious constraint that $w'(z = 0) = 0$. For SN observations, we used wider priors for w and $\Omega_{\rm NR}$ in order to illustrate the differences between the two data sets studied here. We begin with a brief summary of results for the gold + silver data set. The best-fitting model in this case is $w = -1.99$ and $\Omega_{\rm NR} = 0.47$. The allowed range for w at 95 per cent confidence limit for large priors is $-3.73 \leq w \leq -1.25$. The corresponding range for the density parameter is $0.28 \leq \Omega_{\rm NR} \leq 0.57$. With SNLS data, the best-fitting model is $w = -1.06$ and $\Omega_{\rm NR} = 0.29$. The allowed range for w at 95 per cent confidence limit is $-2.36 \leq w \leq -0.74$. The allowed range for the density parameter is $0.11 \leq \Omega_{\rm NR} \leq 0.48$. There is clearly a large shift in the allowed values of parameters.

We illustrate this in Fig. 5 (top left-hand panel) where we have plotted the regions allowed by the two data sets at 68 per cent confidence levels in the w–$\Omega_{\rm NR}$ plane. Dashed line shows the region allowed by the gold + silver data set and the solid line is for the SNLS data set. We can deduce the following from this figure.

(i) The region allowed by these two data sets at 68 per cent confidence level has some overlap, thus we may say that the two sets are consistent with each other.

(ii) The overlap is at $\Omega_{\rm NR} \geq 0.36$ and is thus at margins of what is allowed by other observations.

(iii) The ΛCDM model is ruled out at 68 per cent confidence level by the gold + silver data set.

(iv) The best fit of each set is ruled out by the other data set at this confidence level. Indeed, the best fit of gold + silver data set is allowed by the SNLS data with a probability $\mathcal{P} = 12.65$ per cent while the best fit of the SNLS data set is allowed by the gold + silver data set with $\mathcal{P} = 8.14$ per cent.

This point is reiterated by the likelihoods of w and $\Omega_{\rm NR}$ for these models in the same panel.

The figure shows the large overlap between the likelihood curves corresponding to SNLS and *WMAP* data, where the gold + silver data clearly favour higher values of $\Omega_{\rm NR}$ and more negative w. The phantom models are still allowed but the SNLS data as well as *WMAP* data show a preference for models close to a cosmological constant.

For comparison, *WMAP* allows $-1.25 \leq w \leq -0.7$ and $0.2 \leq \Omega_{\rm NR} \leq 0.38$ if dark energy is assumed to be smooth. If we allow for perturbations in dark energy, then the limits on the equation-of-state parameters changes to $-1.25 \leq w \leq -0.64$ and $0.20 \leq \Omega_{\rm NR} \leq 0.38$ as shown in the top right-hand panel of Fig. 5.

These figures allow us to conclude the following.

(i) *WMAP* observations of temperature and polarization anisotropies strongly favour models around $w = -1$, i.e. the ΛCDM model. As a result, *WMAP* and gold + silver data sets have a small region of overlap as the latter does not favour models around $w = -1$. [It is this disagreement that had led us to suggest that the SN data set could be plagued by some systematic effects (Jassal et al. 2005a), particularly as it contains SNe from a number of different sources. In that paper, we had used *WMAP* first-year data.]

(ii) *WMAP* and SNLS data sets have a region of overlap within 68 per cent confidence levels.

(iii) There is no significant change in the likelihood contours for other cosmological parameters as we go from the cosmological constant model to dark energy with a constant equation-of-state parameter (not constrained to $w = -1$), or when we go from a smooth dark energy to the model where dark energy is allowed to cluster.

Thus we can say that SNLS and *WMAP* data are in (much) better agreement as compared to the gold + silver and *WMAP* data sets.

3.3 Varying $w(z)$

It has been claimed that observations, in particular observations of high-redshift SNe (the gold and gold + silver data sets) favour evolution of dark energy (Alam et al. 2004a,b; Padmanabhan & Choudhury 2003; Jonsson et al. 2004; Jimenez 2003; Amendola & Quercellini 2003; Jimenez et al. 2003; Bassett 2005; Bassett et al. 2004; Corasaniti et al. 2004; Daly & Djorgovski 2005; Gong 2005; Choudhury & Padmanabhan 2005; Wang 2005; Wang et al. 2004).

Table 2. Range of parameters allowed within 95 per cent confidence limit from SNLS, *WMAP*1, *WMAP*3 and SNLS + *WMAP*3.

Parameter	ΛCDM	w = constant	w = constant with perturbations	$p = 1$	$p = 2$	
		−1.92 to −0.74	−1.92 to −0.74	−1.89 to −0.61	−1.9 to −0.59	SNLS
w		−1.39 to −0.58	−1.63 to −0.66	−1.64 to −0.42	−1.93 to −0.43	*WMAP*1
		−1.25 to −0.7	−1.25 to −0.64	−1.62 to −0.44	−1.62 to −0.43	*WMAP*5
		−1.47 to −0.83	−1.57 to −0.88	−1.46 to −0.81	−1.74 to −0.77	SNLS + *WMAP*1
		−1.1 to −0.9	−1.1 to −0.9	−1.3 to −0.8	−1.42 to −0.66	SNLS + *WMAP*5
				−4.82 to 3.3	−4.79 to 4.23	SNLS
$w'(z=0)$				−3.09 to 1.32	−2.5 to 4.87	*WMAP*1
				−1.8 to 1.2	−3.3 to 2.7	*WMAP*5
				−0.99 to 1.04	−2.22 to 4.79	SNLS + *WMAP*1
				−1.25 to 0.91	−2.6 to 2.7	SNLS + *WMAP*5
	0.22–0.31	0.11–0.47	0.11–0.47	0.11–0.48	0.11–0.48	SNLS
$\Omega_{\rm NR}$	0.20–0.45	0.16–0.43	0.20–0.47	0.17–0.45	0.18–0.44	*WMAP*1
	0.19–0.33	0.19–0.38	0.19–0.39	0.19–0.39	0.19–0.38	*WMAP*3
	0.21–0.34	0.2–0.38	0.2–0.38	0.2–0.38	0.20–0.38	*WMAP*5
	0.22–0.31	0.15–0.36	0.18–0.41	0.16–0.38	0.19–0.39	SNLS + *WMAP*1
	0.22–0.3	0.22–0.3	0.22–0.3	0.22–0.33	0.21–0.32	SNLS + *WMAP*5
h	0.61–0.79	0.61–0.78	0.6–0.79	0.6–0.78	0.61–0.78	*WMAP*1
	0.66–0.77	0.60–0.78	0.60–0.78	0.61–0.79	0.61–0.78	*WMAP*5
	0.69–0.77	0.68–0.78	0.68–0.79	0.67–0.77	0.65–0.78	SNLS + *WMAP*1
	0.68–0.74	0.68–0.74	0.68–0.74	0.66–0.76	0.65–0.76	SNLS + *WMAP*5
$\Omega_{\rm B}h^2$	0.02–0.027	0.021–0.028	0.02–0.027	0.02–0.027	0.02–0.027	*WMAP*1
	0.021–0.024	0.021–0.023	0.02–0.024	0.021–0.0235	0.022–0.024	*WMAP*5
	0.02–0.027	0.021–0.027	0.021–0.027	0.021–0.027	0.021–0.028	SNLS + *WMAP*1
	0.021–0.023	0.021–0.024	0.021–0.024	0.021–0.023	0.021–0.024	SNLS + *WMAP*5
n	0.93–1.08	0.93–1.1	0.93–1.09	0.93–1.1	0.93–1.098	*WMAP*1
	0.94–0.99	0.93–0.99	0.93–0.99	0.93–0.99	0.93–0.99	*WMAP*5
	0.93–1.09	0.94–1.08	0.94–1.09	0.93–1.09	0.93–1.097	SNLS + *WMAP*1
	0.94–0.99	0.94–0.99	0.93–0.99	0.93–0.99	0.94–0.99	SNLS + *WMAP*5
τ	0.002–0.33	0.011–0.39	0.007–0.35	0.13–0.4	0.016–0.39	*WMAP*1
	0.054–0.12	0.05–0.12	0.055–0.12	0.054–0.12	0.054–0.12	*WMAP*5
	0.004–0.33	0.008–0.34	0.045–0.37	0.013–0.38	0.017–0.396	SNLS + *WMAP*1
	0.054–0.12	0.053–0.12	0.055–0.13	0.52–0.12	0.05–0.125	SNLS + *WMAP*5

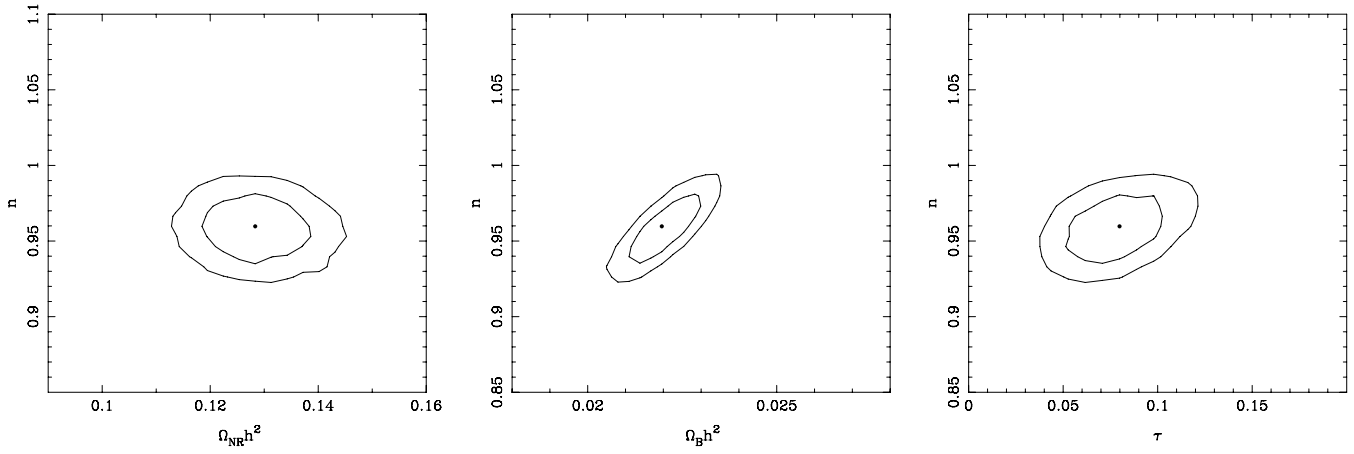

Figure 3. Marginalized likelihood contours for different parameters for ΛCDM model. The regions enclosed by the contours are 68 and 95 per cent confidence limits. The results are consistent with *WMAP*5 results for ΛCDM model. The left-hand plot shows the allowed range in $n - \Omega_{\rm NR}\,h^2$ plane. The next figure shows the correlation between parameters n and $\Omega_{\rm B}\,h^2$. The figure on the right-hand side shows corresponding contours in $n - \tau$ plane.

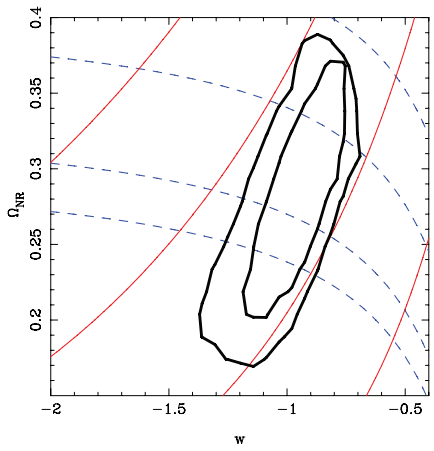

Figure 4. Contours of angular diameter distance (blue/dashed) and of constant angular size of the Hubble radius (red/solid) overlaid with likelihood regions allowed by *WMAP*5 data in the Ω_{NR}–w plane.

As such a variation is impossible if acceleration of the universe is caused by the cosmological constant, it is important to test this claim. Note that the term 'evolution of dark energy' has been used for evolution of the equation-of-state parameter, as well as for evolution of energy density for the dark energy component. In an earlier study using the gold + silver data set, we had found that SN observations *do not* favour evolution of the equation-of-state parameter over models with a constant $w \ll -1$. But these models are favoured strongly as compared to the cosmological constant model, which was allowed with $\mathcal{P} = 6.3$ per cent amongst models with constant w. When combined with *WMAP* and other constraints, the allowed variation of dark energy is restricted to a narrow range and models around the cosmological constant are favoured (Seljak et al. 2005; Jassal et al. 2005a). We should note that if we combine only the gold + silver (or gold) SN and *WMAP* data, then results favour evolution of ρ_{DE}, but adding observations of galaxy clustering removes this inclination.

We studied constraints on models of varying dark energy with the SNLS and *WMAP*5 data and the results are summarized in Table 2, which gives the ranges of parameters allowed at 95 per cent confidence level. The SN data constrain w_0 but do not effectively constrain w_1. On the other hand, CMB data constrain an effective equation of state and hence indirectly provide constraints on $w'(z = 0)$. This is evident from lower panels of Fig. 5, where we have plotted confidence contours in Ω_{NR}–w plane. The CMB contours are significantly narrower than those given by the SN data. We do not find any significant changes in the likelihood contours for other parameters such as n, $\Omega_{NR}h^2$, $\Omega_B h^2$ and τ. For instance the range of

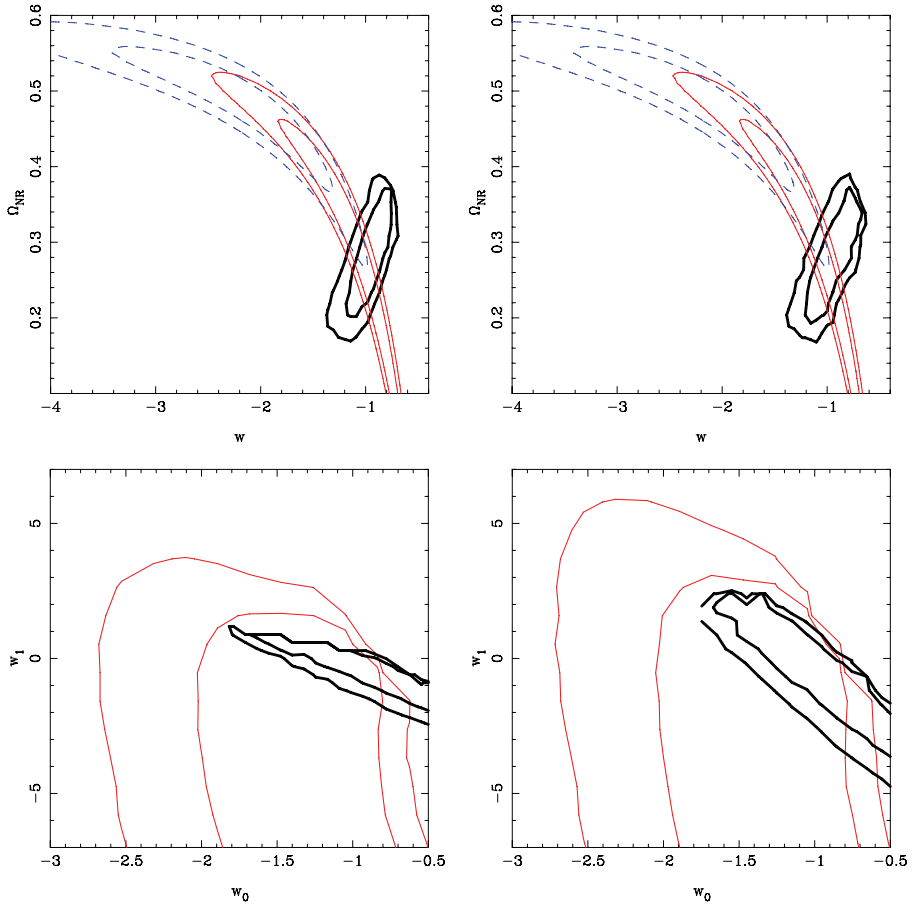

Figure 5. Marginalized likelihood contours in Ω_{NR}–w plane for different models. In the top figures the blue dashed lines correspond to 68 and 95 per cent confidence level using the gold data. The red solid lines correspond to confidence levels in SNLS data. The black thick lines are marginalized confidence levels using *WMAP*5 data. The top left-hand panel is for constant w models with a homogeneous dark energy and the one on the right-hand side is when we include dark energy perturbations. The bottom left-hand plot is for models with $p = 1$ and the right-hand plot is with $p = 2$.

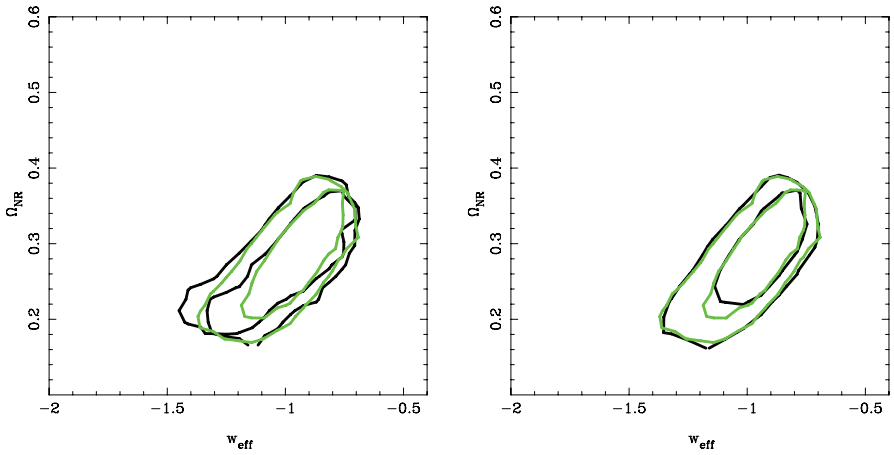

Figure 6. The black (thick solid) contours in this figure show constraints on the effective dark energy equation of state $w_{\rm eff}$ for $p = 1$ and $p = 2$ from the *WMAP*5 data. The green (grey) lines are constraints on constant $w - \Omega_{\rm NR}$ (without perturbations). These clearly show that the CMB data constrain effective equation of state at the last scattering surface.

$\Omega_{\rm NR}h^2$ is given by 0.21–0.33 is valid for all the models considered here. This is illustrated in Table 2.

Given that CMB observations constrain only one number, we expect that the constraint on models with varying $w(z)$ should constrain only $w_{\rm eff}$ as defined in equation (6). We confirm this by plotting likelihood contours for models with varying $w(z)$ on the $\Omega_{\rm NR}$–$w_{\rm eff}$ plane. We also plot contours for constant w models on the same plane for reference. Fig. 6 shows these contours for the models with $p = 1$ and 2. We find very strong coincidence in the contours for models with variable $w(z)$ when plotted with $w_{\rm eff}$ with the contours for models with constant w, thereby confirming our conjecture. This also provides an easy approach to constraining models with variable $w(z)$ without detailed calculations, all that one needs is to check whether $w_{\rm eff}$ is in the range allowed by CMB observations for w in the constant w model.

We return to the issue of variation of dark energy density allowed by observations. A pictorial representation of results is given in Fig. 7, where we have plotted $\rho_{\rm DE}(z)/\rho_{\rm DE}(z = 0)$ as a function of redshift. Different panels show the evolution of this quantity as allowed by the SNLS data set, *WMAP*5 observations of temperature and polarization anisotropies in the CMB and combined constraints from *WMAP*5 + SNLS. These are plotted for constant w (with and without dark energy perturbations), and for variable w with $p = 1$ and 2. Dark energy was assumed to be homogeneous in all cases except for the second row that corresponds to constant w models with perturbations in dark energy. We can conclude the following.

(i) SN observations are a tight constraint for models with constant w, but these are not as strong as CMB constraints.

(ii) SNLS + *WMAP*5 data offer tighter constraints than either data set and the cosmological constant is allowed with a high probability. This follows from the complementary nature of the two constraints as seen from the orientation of the likelihood contours (e.g. see Fig. 5).

(iii) SN observations do not constrain evolution of dark energy density in models with a variable w. Very large variation in dark energy density is allowed by these observations.

(iv) *WMAP*5 observations are, in contrast, a much tighter constraint and do not allow significant variation in dark energy. Indeed, the variation in dark energy density allowed by *WMAP*5 observations for models with variable w is not significantly larger than that allowed for constant w models.

(v) We demonstrate that the constraints on dark energy parameters for varying w models are the same as the constraints on constant w models if we consider $w_{\rm eff}$ for varying dark energy models.

(vi) SNLS + *WMAP* constraints are essentially dominated by the *WMAP* data and follow the same pattern. SNLS observations add to the overall constraint by limiting the range of values allowed for w_0.

We would like to add a note of caution that the analysis for varying w models does not take perturbations in dark energy into account. However, these are more important for $w \gg -1$ or models with rapidly varying w (Bean & Doré 2004; Caldwell et al. 1998; Weller & Lewis 2003; Hannestad 2005) and such models are not allowed by observational constraints.

4 DISCUSSION

In this paper we studied the SNLS data set and compared the constraints obtained with constraints from *WMAP*5 data on temperature anisotropies in the CMB. We find that the parameter values favoured by the two data sets have significant overlap and the two sets can be combined to put tight constraints on models of dark energy. In an earlier work we had noted that the gold + silver data set does not agree with *WMAP* observations in that these favour distinct parts of the parameter space (Jassal et al. 2005a). Constraints from *WMAP* and structure formation favour similar models, but ones distinct from those favoured by gold + silver SN observations. This indicates some degree of inconsistency between the SN and other observations and it led us to suggest that the gold + silver data set may be affected by as yet unknown systematic errors (Jassal et al. 2005a). One reason for doubting the SN data is the heterogeneity of sources from which the particular data set was collected (Riess et al. 2004). SNLS (Astier et al. 2005) is a homogeneous data set and should not suffer from such problems and indeed we find that there is no inconsistency between SNLS and *WMAP* observations.

This highlights the usefulness of CMB observations for constraining models of dark energy (Eisenstein & White 2004; Jassal et al. 2005). We believe that CMB observations should be used for testing any model of dark energy as SN observations do not constrain models with varying w effectively.[3] Thus one should use

[3] The main constraint on varying w models is from the CMB data.

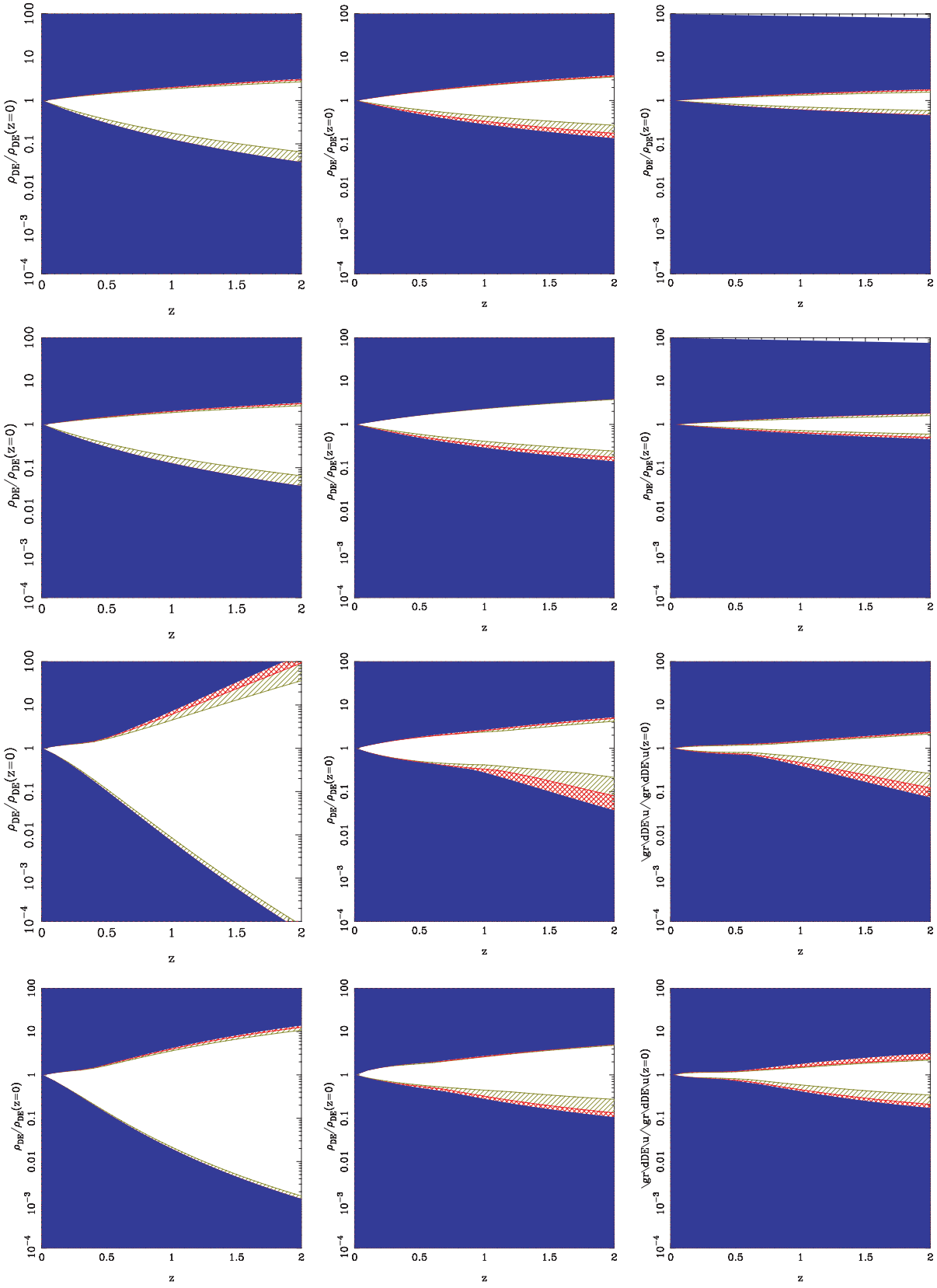

Figure 7. The allowed range in variation of dark energy density as a function of redshift. The top row is for homogeneous dark energy model, the second row is for perturbed dark energy, the third row is for varying w with $p = 1$, and, the last row is for varying w with $p = 2$. The white region is the allowed range at 63 per cent confidence level, the hatched region is the one disallowed range of dark energy density at 95 per cent confidence level and the solid (blue) region is the one ruled out at 99 per cent confidence level. In all the rows, the leftmost plot shows range allowed by SNLS data, the middle one with *WMAP*5 data and the right-hand one shows the range allowed by combined data.

CMB observations as well and not rely only on SN observations for constraining such models.

We would like to add a note of caution against combining the SNLS data with other data sets of high-redshift SNe in light of the very different nature of these data sets. Indeed, one should use homogeneous data sets like the SNLS in isolation to avoid the problems mentioned above.

In terms of models, we find that the cosmological constant is favoured by individual observations (SNLS and *WMAP*) as well as in the combined data set with very high probability. Table 2 gives allowed values of all cosmological parameters at 95 per cent confidence level by SNLS, *WMAP* as well as the combined data set. For the cases where a similar analysis has been done by others, our results are consistent with other findings (Bridle et al. 2003; Spergel et al. 2003; Maccio et al. 2004; Linder & Jenkins 2003; Pogosyan, Bond & Contaldi 2003; Tegmark et al. 2004; Wang & Tegmark 2004; Giovi, Baccigalupi & Perrotta 2005; Hannestad 2004; Huterer & Cooray 2005; Lee 2005; Lee & Ng 2003; Lee, Lee & Ng 2005; Mainini, Colombo & Bonometto 2005; Rapetti, Allen & Weller 2005; Pogosian 2005; Nesseris & Perivolaropoulos 2006; Seljak et al. 2005; Shen et al. 2005; Feng, Wang & Zhang 2005; Xia et al. 2006a,b; Amendola, Campos & Rosenfeld 2007; Calvo & Maroto 2006; Carneiro et al. 2006; Dantas et al. 2007; Elizalde et al. 2008; Mota et al. 2007).

We have discussed the origin of the constraint on dark energy models from CMB observations at length. We may conclude the following from the analysis presented here.

(i) Location of acoustic peaks in the angular power spectrum of CMB anisotropies is the main source of constraints.

(ii) CMB observations only constrain $w_{\rm eff}$, an effective value of the equation-of-state parameter defined in equation (6). This can be used to translate constraints on models with constant w to models where dark energy properties vary with time.

(iii) We have discussed models with $\Omega_0 = 1$ in this paper. In case this constraint is relaxed, then the well-known degeneracy between w and Ω_0 loosens the constraints. However, it is well known that the SN and CMB data are complementary and can be combined to provide fairly tight constraints even in this case (Perlmutter, Turner & White 1999; Huterer & Turner 2001). We do not expect variations in curvature to modify our conclusions about $w_{\rm eff}$ being the only dark energy related quantity constrained by CMB observations.

(iv) ISW effect due to perturbations in dark energy can, in principle, lead to variations in the CMB radiation angular power spectrum at small l. Our analysis of models with variable w without perturbations does not take this into account. Various analyses have shown that ISW does not contribute significantly to constraining cosmological parameters from CMB data (see e.g. Xia et al. 2009). The main reason for this is that ISW affects power at small l, and due to large cosmic variance these modes do not contribute much to the overall likelihood.

ACKNOWLEDGMENTS

Numerical work for this paper was carried out at cluster computing facility in the Harish-Chandra Research Institute (http://cluster.hri.res.in). This research has made use of NASA's Astrophysics Data System. HKJ thanks the Department of Science and Technology, India for financial assistance through project number SR/WOS-A/PS-11/2006.

REFERENCES

Aguirregabiria J. M., Lazkoz R., 2004, Phys. Rev. D, 69, 123502
Alam U., Sahni V., Starobinsky A. A., 2004a, J. Cosmol. Astropart. Phys., 0406, 008
Alam U., Saini T. D., Sahni V., Starobinsky A. A., 2004b, MNRAS, 354, 275
Alcaniz J. S., 2006, Brazilian J. Phys., 36, 1109
Amendola L., Quercellini C., 2003, Phys. Rev. D, 68, 023514
Amendola L., Campos G. C., Rosenfeld R., 2007, Phys. Rev. D, 75, 083506
Andrianov A. A., Cannata F., Kamenshchik A. Y., 2005, Phys. Rev. D, 72, 043531
Apostolopoulos P. S., Tetradis N., 2006, Phys. Rev. D, 74, 064021
Arianto, Zen, F. P., Gunara B. E., Triyanta, Supardi, 2007, J. High Energy Phys., 9, 48
Armendariz-Picon C., Mukhanov V., Steinhardt P. J., 2001, Phys. Rev. D, 63, 103510
Astier P. et al., 2005, preprint (astro-ph/0510447)
Bagla J. S., Padmanabhan T., Narlikar J. V., 1996, Comments Astrophys., 18, 275
Bagla J. S., Jassal H. K., Padmanabhan T., 2003, Phys. Rev. D, 67, 063504
Barris B. J. et al., 2004, ApJ, 602, 571
Bartolo N., Corasaniti P.-S., Liddle A. R., Malquarti M., 2004, Phys. Rev. D, 70, 043532
Bassett B. A., 2005, Phys. Rev. D, 71, 083517
Bassett B. A., Corasaniti P. S., Kunz M., 2004, ApJ, 617, L1
Bean R., Doré O., 2004, Phys. Rev. D, 69, 083503
Benabed K., Bernardeau F., 2001, Phys. Rev. D, 64, 083501
Bento M. C., Bertolami O., Sen A. A., 2002, Phys. Rev. D, 66, 043507
Bludman S. A., Roos M., 2002, Phys. Rev. D, 65, 043503
Bridle S. L., Lahav O., Ostriker J. P., Steinhardt P. J., 2003, Sci, 299, 1532
Briscese F., Elizalde E., Nojiri S., Odintsov S. D., 2007, Phys. Lett. B, 646, 105
Bronnikov K. A., Starobinsky A. A., 2007, J. Exp. Theor. Phys. Lett., 85, 1
Bronnikov K. A., Fabris J. C., Gonçalves S. V. B., 2007, J. Phys. A, 40, 6835
Burgess C. P., 2003, Int. J. Modern Phys. D, 12, 1737
Caldwell R. R., 2002, Phys. Lett. B, 545, 23
Caldwell R. R., Dave R., Steinhardt P. J., 1998, Phys. Rev. Lett. 80, 1582
Calvo G. B., Maroto A. L., 2006, Phys. Rev. D, 74, 083519
Carneiro S., Pigozzo C., Borges H. A., Alcaniz J. S., 2006, Phys. Rev. D, 74, 023532
Carroll S. M., Press W. H., Turner E. L., 1992, ARA&A, 30, 499
Carroll S. M., Hoffman M., Trodden M., 2003, Phys. Rev. D, 68, 023509
Chiba T., 2002, Phys. Rev. D, 66, 063514
Chimento L. P., Feinstein A., 2004, Modern Phys. Lett. A, 19, 761
Choudhury T. R., Padmanabhan T., 2005, A&A, 429, 807
Choudhury D., Ghoshal D., Jatkar D. P., Panda S., 2002, Phys. Lett. B, 544, 231
Clarkson C., Cortês M., Bassett B., 2007, J. Cosmol. Astropart. Phys., 8, 11
Cline J. M., Jeon S. Y., Moore G. D., 2004, Phys. Rev. D, 70, 043543
Cognola G., Elizalde E., Nojiri S., Odinstov S. D., Zerbini S., 2006, Phys. Rev. D, 73, 084007
Copeland E. J., Sami M., Tsujikawa S., 2006, Int. J. Modern Phys. D, 15, 1753
Corasaniti P. S., Kunz M., Parkinson D., Copeland E. J., Bassett B. A., 2004, Phys. Rev. D, 70, 083006
Dabrowski M. P., Stachowiak T., Szydlowski M., 2003, Phys. Rev. D, 68, 103519
Daly R. A., Djorgovski S. G., 2005, Int. J. Modern Phys., 20, 1113
Dantas M. A., Alcaniz J. S., Jain D., Dev A., 2007, A&A, 467, 421
Das S., Banerjee N., Dadhich N., 2006, Classical Quantum Gravity, 23, 4159
de la Macorra A., Piccinelli G., 2000, Phys. Rev. D, 61, 123503
de Ritis R., Marino A. A., 2001, Phys. Rev. D, 64, 083509
Dev A., Jain D., Alcaniz J. S., 2003, Phys. Rev. D, 67, 023515
Doran M., Robbers G., 2006, J. Cosmol. Astropart. Phys., 6, 26

Dunkley J. et al., 2008, ApJS, 180, 306
Efstathiou G., Sutherland W. J., Maddox S. J., 1990, Nat, 348, 705
Eisenstein D. J., White M., 2004, Phys. Rev. D, 70, 103523
Elizalde E., Nojiri S., Odintsov S. D., 2004, Phys. Rev. D, 70, 043539
Elizalde E., Nojiri S., Odintsov S. D., Sáez-Gómez D., Faraoni V., 2008, Phys. Rev. D, 77, 106005
Ellis J. R., 2003, Philos. Trans. R. Soc. Lond. A, 361, 2607
Fabris J. C., Gonçalves S. V. B., 2006, Phys. Rev. D, 74, 027301
Fabris J. C., Shapiro I. L., Solà J., 2007, J. Cosmol. Astropart. Phys., 2, 16
Feng B., Wang X., Zhang X., 2005, Phys. Lett. B, 607, 35
Frampton P. H., 2004, Mod. Phys. Lett. A, 19, 801
Frolov A. V., Kofman L., Starobinsky A. A., 2002, Phys. Lett. B, 545, 8
Garnavich P. M. et al., 1998, ApJ, 509, 74
Gibbons G. W., 2002, Phys. Lett. B, 537, 1
Gibbons G. W., 2003, Classical Quantum Gravity, 20, S321
Gibbons G. W., preprint (hep-th/0302199)
Giovi F., Baccigalupi C., Perrotta F., 2005, Phys. Rev. D, 71, 103009
Gong Y. G., 2005, Int. J. Modern Phys. D, 14, 599
Gonzalez-Diaz P. F., 2000, Phys. Lett. B, 481, 353
Gonzalez-Diaz P. F., 2002, Phys. Rev. D, 62, 023513
Gonzalez-Diaz P. F., 2003, Phys. Rev. D, 68, 021303
Gordon C., Hu W., 2004, Phys. Rev. D, 70, 083003
Gordon C., Wands D., 2005, Phys. Rev. D, 71, 123505
Gorini V., Kamenshchik A. Y., Moschella U., Pasquier V., 2001, Phys. lett. B, 511, 265
Gorini V., Kamenshchik A. Y., Moschella U., Pasquier V., 2004, Phys. Rev. D, 69, 123512
Gupta S., Saini T. D., Laskar T., 2009, preprint (astro-ph/0701683)
Hannestad S., 2004, J. Cosmol. Astropart. Phys., 0409, 001
Hannestad S., 2005, Phys. Rev. D, 71, 103519
Hannestad S., Mortsell E., 2004, J. Cosmol. Astropart. Phys., 0409, 001
Hao J. g. Li X. z., 2003, Phys. Rev. D, 67, 107303
Holman R., Naidu S., 2004, preprint (astro-ph/0408102)
Hu W., 2005, Phys. Rev. D, 71, 047301
Hu W., Dodelson S., 2002, ARA&A, 40, 171
Huterer D., Turner M. S., 2001, Phys. Rev. D, 64, 123527
Huterer D., Cooray A., 2005, Phys. Rev. D, 71, 023506
Jain P., Ralston J. P., 2006, ApJ, 637, 91
Jassal H. K., 2004, Pramana, 62, 757
Jassal H. K., Bagla J. S., Padmanabhan T., 2005, Phys. Rev. D, 72, 103503
Jassal H. K., Bagla J. S., Padmanabhan T., 2005, MNRAS, 356, L11
Jassal H. K., 2009, Phys. Rev. D, 79, 127301
Jassal H. K., preprint (hep-th/0312253)
Jimenez R., 2003, New Astron. Rev., 47, 761
Jimenez R., Verde L., Treu T., Stern D., 2003, ApJ, 593, 622
Jonsson J., Goobar A., Amanullah R., Bergstrom L., 2004, J. Cosmol. Astropart. Phys., 0409, 007
Kim C., Kim H. B., Kim Y. B., 2003, Phys. Lett. B, 552, 111
Komatsu E. et al., 2009, ApJS, 180, 330
Kowalski M. et al., 2008, ApJ, 686, 749
Lazkoz R., Nesseris S., Perivolaropoulos L., 2005, J. Cosmol. Astropart. Phys., 11, 10
Lee W., Ng K., 2003, Phys. Rev. D, 67, 107302
Lee S., 2005, Phys. Rev. D, 71, 123528
Lee D.-S., Lee W., Ng K., 2005, Int. J. Modern Phys. D, 14, 335
Li M., 2004, Phys. Lett. B, 603, 1
Linder E. V., Jenkins A., 2003, MNRAS, 346, 573
Linder E. V., Robbers G., 2008, J. Cosmol. Astropart. Phys., 0806, 004
Maccio A. V., Bonometto S. A., Mainini R., Klypin A., 2004, ASSL, 301, 199
Mainini R., 2008, J. Cosmol. Astropart. Phys., 0807, 003
Mainini R., 2009, J. Cosmol. Astropart. Phys., 0904, 017
Mainini R., Colombo P. L., Bonometto S. A., 2005, ApJ, 632, 691
Malquarti M., Copeland E. J., Liddle A. R., Trodden M., 2003, Phys. Rev. D, 67, 123503
Melchiorri A. et al., (Boomerang Collaboration), 2000, ApJ, 536, L63
Milton K. A., 2003, Gravitation Cosmology, 9, 66
Mota D. F., van de Bruck C., 2004, A&A, 421, 71
Mota D. F., Kristiansen J. R., Koivisto T., Groeneboom N. E., 2007, MNRAS, 382, 793
Nesseris S., Perivolaropoulos L., 2005, Phys. Rev. D, 72, 123519
Nojiri S., Odintsov S. D., 2003, Phys. Lett. B, 562, 147
Nojiri S., Odintsov S. D., Tsujikawa S., 2005, Phys. Rev. D, 71, 063004
Nunes N. J., Mota D. F., 2006, MNRAS, 368, 751
Onemli V. K., Woodard R. P., 2002, Classical Quantum Gravity, 19, 4607
Onemli V. K., Woodard R. P., 2004, Phys. Rev. D, 70, 107301
Ostriker J. P., Steinhardt P. J., 1995, Nat, 377, 600
Padmanabhan T., 2002, Phys. Rev. D, 66, 021301
Padmanabhan T., 2002, Classical Quantum Gravity, 19, 5387
Padmanabhan T., 2003, Phys. Rep., 380, 235
Padmanabhan T., 2005a, Curr. Sci., 88, 1057
Padmanabhan T., 2005b, Space-Time Structure: Einstein and Beyond. World Scientific, Singapore
Padmanabhan T., 2005c, Phys. Rep. 49, 406
Padmanabhan T., 2005d, preprint (astro-ph/0510492)
Padmanabhan T., 2005e, Int. J. Modern Phys. D, 14, 2263
Padmanabhan T., Choudhury T. R., 2003, MNRAS, 344, 823
Peebles P. J. E., Ratra B., 2003, Rev. Modern Phys., 75, 559
Peiris H. V., Spergel D. N., 2000, ApJ, 540, 605
Percival W. J. et al., 2007, ApJ, 657, 645
Perivolaropoulos L., 2006, preprint (astro-ph/0601014)
Perlmutter S., Schmidt B. P., 2003, Lect. Notes Phys., 598, 195
Perlmutter S. et al., 1999, ApJ, 517, 565
Perlmutter S., Turner M. S., White M., 1999, Phys. Rev. Lett., 83, 670
Pogosian L., 2005, J. Cosmol. Astropart. Phys., 4, 15
Pogosyan D., Bond J. R., Contaldi C. R., preprint (astro-ph/0301310)
Polarski D., Ranquet A., 2005, Phys. Lett. B, 627, 1
Rapetti D., Allen S. W., Weller J., 2005, MNRAS, 360, 555
Ren J., Meng X., 2006, Phys. Lett. B, 633, 1
Riess A. G. et al., 1998, AJ, 116, 1009
Riess A. G. et al., 2004, ApJ, 607, 665
Rubano C., Scudellaro P., 2002, Gen. Relativ. Gravitation, 34, 307
Sahni V., Shtanov Y., 2003, J. Cosmol. Astropart. Phys., 0311, 014
Sahni V., Starobinsky A. A., 2000, Int. J. Modern Phys. D, 9, 373
Sahni V., Shafieloo A., Starobinsky A., 2008, Phys. Rev. D, 78, 103502
Scherrer R. J., 2004, Phys. Rev. Lett., 93, 011301
Seljak U., Zaldarriaga M., 1996, ApJ, 469, 437
Seljak U. et al., 2005, Phys. Rev. D, 71, 103515
Sen A., 2005, Phys. Scr. T, 117, 70
Sen A. A., Scherrer R. J., 2005, Phys. Rev. D, 72, 063511
Sen S., Seshadri T. R., 2003, Int. J. Modern Phys. D, 12, 445
Sergijenko O., Kulinich Y., Novosyadlyj B., Pelykh V., 2008, preprint (arXiv:0809.3349)
Shen J., Wang B., Abdalla E., Su R., 2005, Phys. Lett. B, 609, 200
Shiu G., Wasserman I., 2002, Phys. Lett. B, 541, 6
Singh P., Sami M., Dadhich N., 2003, Phys. Rev. D, 68, 023522
Sola J., Stefancic H., 2006, Mod. Phys. Lett. A, 21, 479
Spergel D. N. et al., 2003, ApJS, 148, 175
Steinhardt P. J., 2003, Philos. Trans. R. Soc. Lond. A, 361, 2497
Subramanian K., preprint (astro-ph/0411049)
Tegmark M. et al., 2004, ApJ, 606, 702
Tonry J. L. et al., 2003, ApJ, 594, 1
Unnikrishnan S., Jassal H. K., Seshadri T. R., 2008, Phys. Rev. D, 78, 123504
Urena-Lopez L. A., Matos T., 2000, Phys. Rev. D, 62, 081302
Uzawa K., Soda J., 2001, Modern Phys. Lett. A, 16, 1089
Virey J.-M., Taxil P., Tilquin A., Ealet A., Tao C., Fouchez D., 2005, Phys. Rev. D, 72, 061302
Wang Y., 2005, New Astron. Rev., 49, 97
Wang Y., Tegmark M., 2004, Phys. Rev. Lett., 92, 241302
Wang Y., Kostov V., Freese K., Frieman J. A., Gondolo P., 2004, J. Cosmol. Astropart. Phys., 12, 3

Weinberg S., 1989, Rev. Modern Phys., 61, 1
Weller J., Lewis A. M., 2003, MNRAS, 346, 987
White M., Cohn J. D., preprint (astro-ph/0203120)
Wood-Vasey W. M. et al., 2007, ApJ, 666, 694
Xia J., Zhao G., Feng B., Li H., Zhang X., 2006a, Phys. Rev. D, 73, 063521
Xia J., Zhao G., Li H., Feng B., Zhang X., 2006b, Phys. Rev. D, 74, 083521
Xia J., Li H., Zhao G., Zhang X., 2008, Phys. Rev. D, 78, 0835254
Xia J.-Q., Viel M., Baccigalupi C., Matarrese S., 2009, J. Cosmol. Astropart. Phys., 9, 3

This paper has been typeset from a TEX/LATEX file prepared by the author.